Am J Cancer Res 2018;8(2):302-316
www.ajcr.us /ISSN:2156-6976/ajcr0072734

Original Article

Cancer-associated fibroblasts promote stem cell-like properties of hepatocellular carcinoma cells through IL-6/STAT3/Notch signaling

Si Xiong[1], Ronghua Wang[1], Qian Chen[1], Jing Luo[2], Jinlin Wang[1], Zhenxiong Zhao[1], Yawen Li[1], Yun Wang[1], Xiju Wang[1], Bin Cheng[1]

Departments of [1]Gastroenterology and Hepatology, [2]Emergency, Tongji Hospital, Tongji Medical College, Huazhong University of Science and Technology, Wuhan 430030, PR China

Received January 14, 2018; Accepted January 30, 2018; Epub February 1, 2018; Published February 15, 2018

Abstract: In this study, we investigated the role of cancer-associated fibroblasts (CAFs) in hepatocellular carcinoma (HCC) progression. We showed that CAFs secrete high levels of IL-6, which promoted stem cell-like properties in HCC cells by activating Notch signaling through STAT3 Tyr705 phosphorylation. These effects were abolished by Notch1 shRNA knockdown in HCC cells or treatment with an IL-6 neutralizing antibody or the p-STAT3 (Tyr705) inhibitor cryptotanshinone. Xenografted liver tumors were larger in nude mice injected with HCC cells and CAFs than in those receiving HCC cells alone. Moreover, immunohistochemical analysis of liver tissue specimens from 88 HCC patients revealed that high nuclear Notch intracellular domain (nNICD) levels in HCC cells correlated with poor prognosis in patients. These findings suggest that IL-6 secreted by CAFs promotes stem cell-like properties in HCC cells by enhancing STAT3/Notch signaling.

Keywords: Cancer-associated fibroblasts, hepatocellular carcinoma, cancer stem cells, notch signaling, IL-6

Introduction

Human hepatocellular carcinoma (HCC) is the sixth most prevalent cancer and third leading cause of cancer deaths worldwide [1]. Cancer stem cells (CSCs) are related to poor outcomes in HCC patients because they have a high potential for tumor initiation and progression [2, 3]. Previous studies have indicated that cancer cell may re-enter a stem cell state and subsequently acquires a CSC phenotype in the tumor microenvironment. This plastic character and so-called dedifferentiation of tumor cells may play important roles in tumorigenesis [4-7].

Tumor cells reside in a tumor microenvironment (TME), which is made up of extracellular matrix (ECM), antigenic vascular cells (AVCs), infiltrating immune cells (IICs), and cancer-associated fibroblasts (CAFs) [6]. CAFs are rich in the tumor microenvironment of HCC, as most HCC cases occur in fibrotic or cirrhotic livers, which are always accompanied by an enrichment of myofibroblasts derived from quiescent fibroblasts and hepatic stellate cells [8-10]. CAFs secrete a variety of cytokines, which promote cancer growth and progression [4, 6, 8, 11-16]. CAFs enhance migration and EMT of gastric cancer cells by secreting IL-6 [14]. They produce TGF-β and SDF1, which promote vascular mimicry formation in HCC [16]. CAFs also promote CSCs through IGF-II signaling in lung cancer [4] and CCL2-Notch signaling in breast cancer [12]. Notch signaling promotes self-renewal and proliferation of CSCs in many cancers [17-20]. In a previous study, we demonstrated that Notch signaling promotes CSC characteristics of CD90+ cells in HCC [21]. However, the mechanisms by which CAFs induce stem cell-like characteristics in HCC cells are not well understood. Therefore, we investigated the mechanisms by which CAFs induce stemness in HCC cells.

Materials and methods

Patient liver tissue specimen and demographic information

We obtained paraffin-embedded sections of HCC and adjacent liver specimens from 88 HCC

patients that underwent curative resection between 2013 and 2016 at the Tongji Hospital, Huazhong University of Science and Technology (HUST, Wuhan, China). Clinical data associated with these specimens were recorded without patient identification. All human experiments were approved by the ethics committee of Tongji Hospital. Informed consent was obtained from all subjects. The patients were enrolled as described previously [22]. Tumor differentiation was defined according to the Edmondson grading system.

Cell culture

Human HCC cell lines, PLC/PRF/5 was obtained from the American Type Culture Collection (ATCC, Manassas, VA, USA) and MHCC-97H was obtained from the Cell Bank of the Chinese Academy of Sciences (Shanghai, China). The human HCC cell line, HLE, was obtained from the Japanese Cancer Research Bank (Tokyo, Japan). All cell lines were cultured in Dulbecco's modified Eagle's medium (DMEM; GIBCO, Grand Island, NY, USA) supplemented with 10% fetal bovine serum (FBS; GIBCO) at 37°C and 5% CO_2.

Isolation and purification of CAFs and peritumor fibroblasts (PTFs)

Human HCC tissues and adjacent normal liver tissues were minced into 2-3-mm fragments, washed in D-Hanks solution with 2% penicillin/streptomycin, and plated in a petri dish with DMEM containing 15% fetal bovine serum and 2% penicillin/streptomycin. Fibroblasts were allowed to grow out of tumor fragments for 1-2 weeks at 37°C and 5% CO_2. We obtained 95% purified fibroblasts after 2-3 passages. These cells were tested for the expression of vimentin, fibroblast activation protein (FAP), and α-SMA by immunofluorescence and western blotting. We used CAFs and PTFs from passages 3-10 for the various experiments. The established CAFs were from five patients.

Sphere formation assay

Sphere formation assay is described in the Supplementary Materials and Methods section.

Immunohistochemistry

Immunohistochemical staining was performed on formalin-fixed, paraffin-embedded liver tissue sections by the labelled streptavidin biotin peroxidase complex method. Patient sample sections were stained with the primary rabbit monoclonal anti-activated Notch1 antibody (cat# ab8925; Abcam, Cambridge, UK) according to the manufacturer's instructions. The intensity of staining was scored on a four-point scale as negative (-), weak (+), moderate (++), or strong (+++). The percentage of positively stained tumor area relative to the entire tumor area was scored on a scale of 0 to 4, 0 (0%), 1 (1-25%), 2 (26-50%), 3 (51-75%), and 4 (76-100%) [23]. An overall protein expression score (range 0-12) was calculated by multiplying the staining intensity and positive staining scores as described previously [24]. Scores ≤ 4 denoted low expression, whereas scores ≥ 5 denoted high expression. All slides were scored by pathologists.

Mouse xenograft tumor assay

All experiments with mice were approved by the Animal Care and Use Committee of Tongji Hospital. We obtained 4-5 week old male NOD/SCID mice from Beijing Huafukang Bioscience and maintained in pathogen-free conditions. We resuspended HCC cells with or without CAFs in serum-free medium, mixed with matrigel in a 1:1 ratio and injected into the liver or subcutaneous tissue of NOD/SCID mice. Mice were monitored for 8 weeks, and the incidences of tumor formation and metastasis were examined and scored. The different groups of mice and the number of mice analyzed per group are presented in the supplementary section (Table S2).

Lentiviral-based knockdown of Notch signaling

For suppression of Notch in HCC cells, lentiviral particles (Genechem, Shanghai, China) expressing Notch1-shRNA were used to regulate Notch signalling in sorted HCC cells. The siRNA sequence specifically targeting Notch1 was as follows: 5'-GGAGCATGTGTAACATCAA-3'. We generated lentiviral particles (Genechem, Shanghai, China) expressing Notch1-shRNA to suppress Notch signaling in HCC cells. Then, HCC cells were infected with Lv-Notch1-shRNA at different multiplicities of infection (MOIs) for 12 h in the presence of 5 μg/ml polybrene. Three days after infection, the expression of green fluorescence protein (GFP) was measured analyzed by flow cytometry. MOI of 10 resulted in more than 90% infection efficiency without

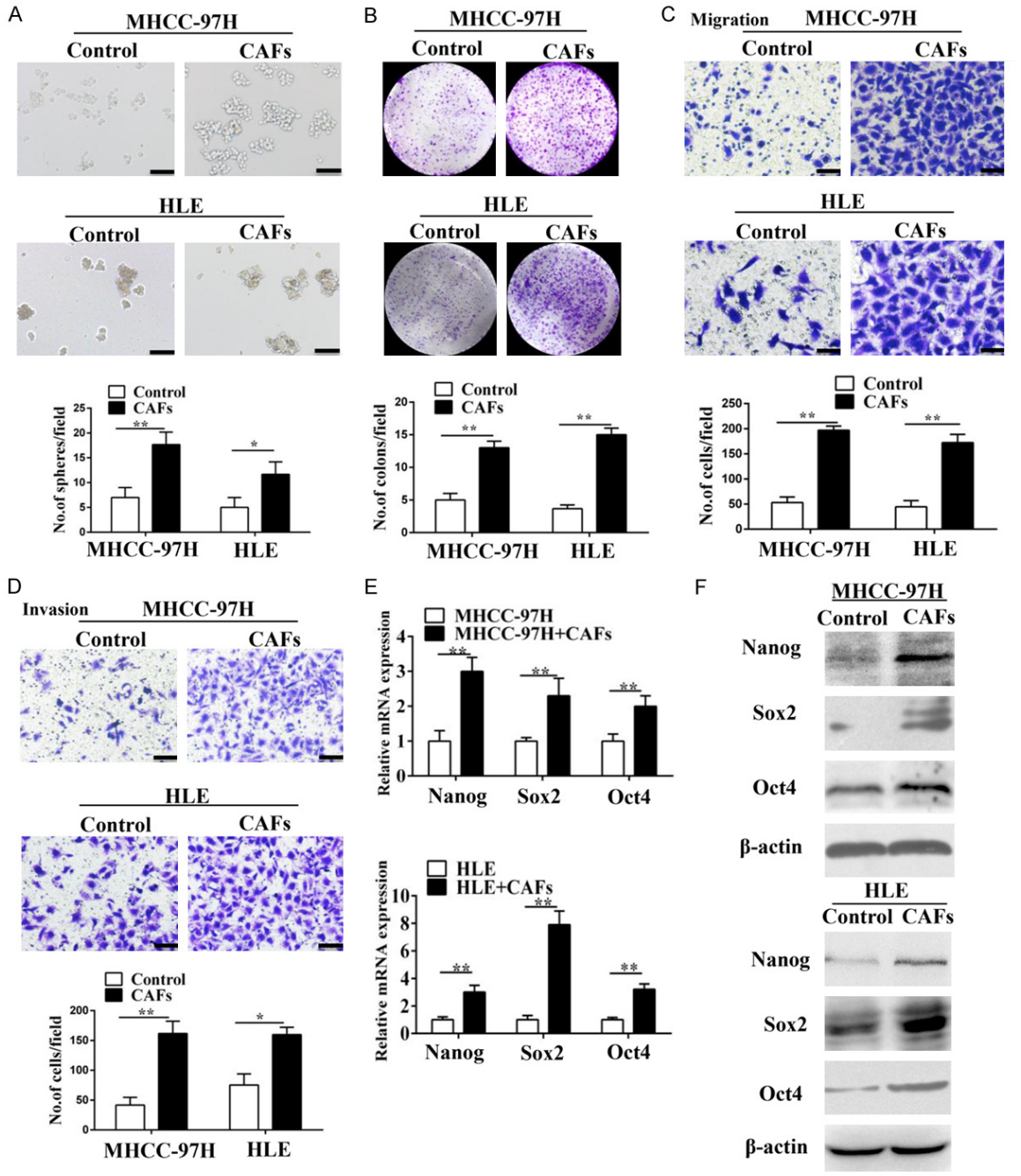

Figure 1. CAFs promote the stem cell-like properties of HCC cells in vitro. (A-D) CAFs enhanced the sphere-forming (A), colony-forming (B), and migration (C) and invasion (D) abilities of MHCC-97H cells and HLE cells. Scale bar, 100 μm. (E and F) RT-PCR (E) and western blotting (F) of stemness-associated genes (Nanog, Sox2 and Oct4) overexpressed in MHCC-97H and HLE cells co-cultured with CAFs. Data are shown as the means ± SD from at least three independent experiments. (*P < 0.05, **P < 0.01).

damaging cells [21] and was used for the experiments.

Quantitative RT-PCR

Quantitative RT-PCR was conducted as previously described [9, 25]. The assay details and primer sequences (Table S3) are presented in the Supplementary section.

Western blotting

Western blot analysis was performed as described previously [21]. Primary antibodies for Notch1 (cat#3608), Hes1 (cat#11988), Nanog (cat#4903), Sox2 (cat#3579), Oct4 (cat#2750), STAT3 (cat#8768), and p-STAT3 (cat#9145) were purchased from Cell Signaling

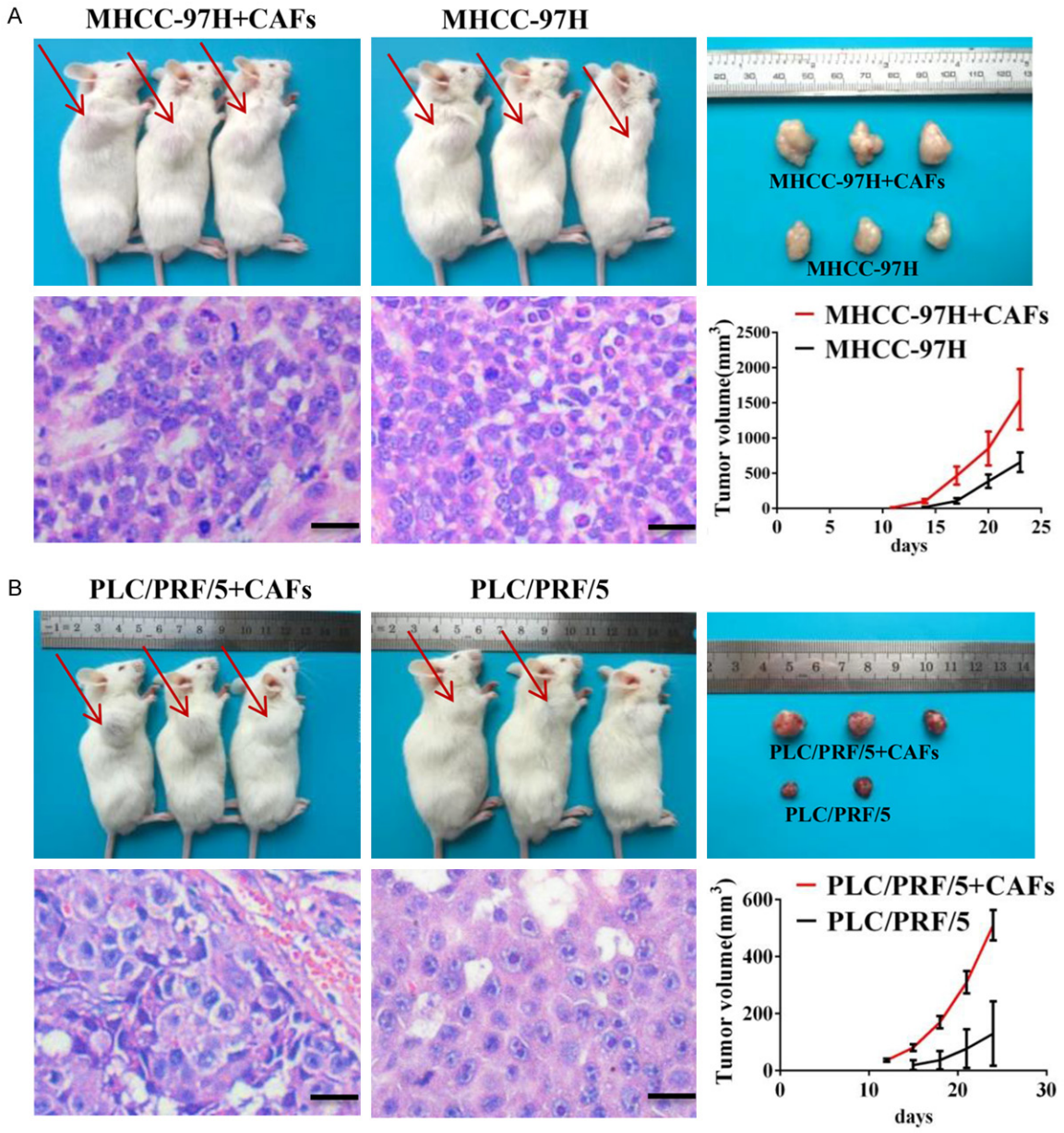

Figure 2. CAFs promote the stem cell-like properties of HCC cells in vivo. MHCC-97H cells (A) or PLC/PRF/5 (B) cells were subcutaneously injected into NOD/SCID mice alone or with CAFs. MHCC-97H cells (A) or PLC/PRF/5 (B) injected with CAFs formed a greater number of larger tumors compared to tumor cells injected alone. Paraffin-embedded tissues of xenotransplanted tumors were processed for H&E staining. Scale bar, 50 μm. Red arrow indicates the site of tumor formation for MHCC-97H cells.

Technology, Inc. (Danvers, MA, USA). Monoclonal mouse anti-β-actin (cat#ab8226; Abcam) was used as an internal control.

Statistical analysis

All statistical analyses were performed with the SPSS (v20.0; SPSS, Inc., Chicago, IL, USA) software. Student's t-test was used for two-group comparisons. Chi-square (χ^2) tests and Fisher's exact tests (for nominal variables) were used for analyzing clinical parameters. The data is presented as mean ± standard deviation. $P < 0.05$ was considered statistically significant.

Results

CAFs promote stem cell-like properties of HCC cells

We showed higher levels of α-SMA, FAP, and vimentin in cancer-associated fibroblasts

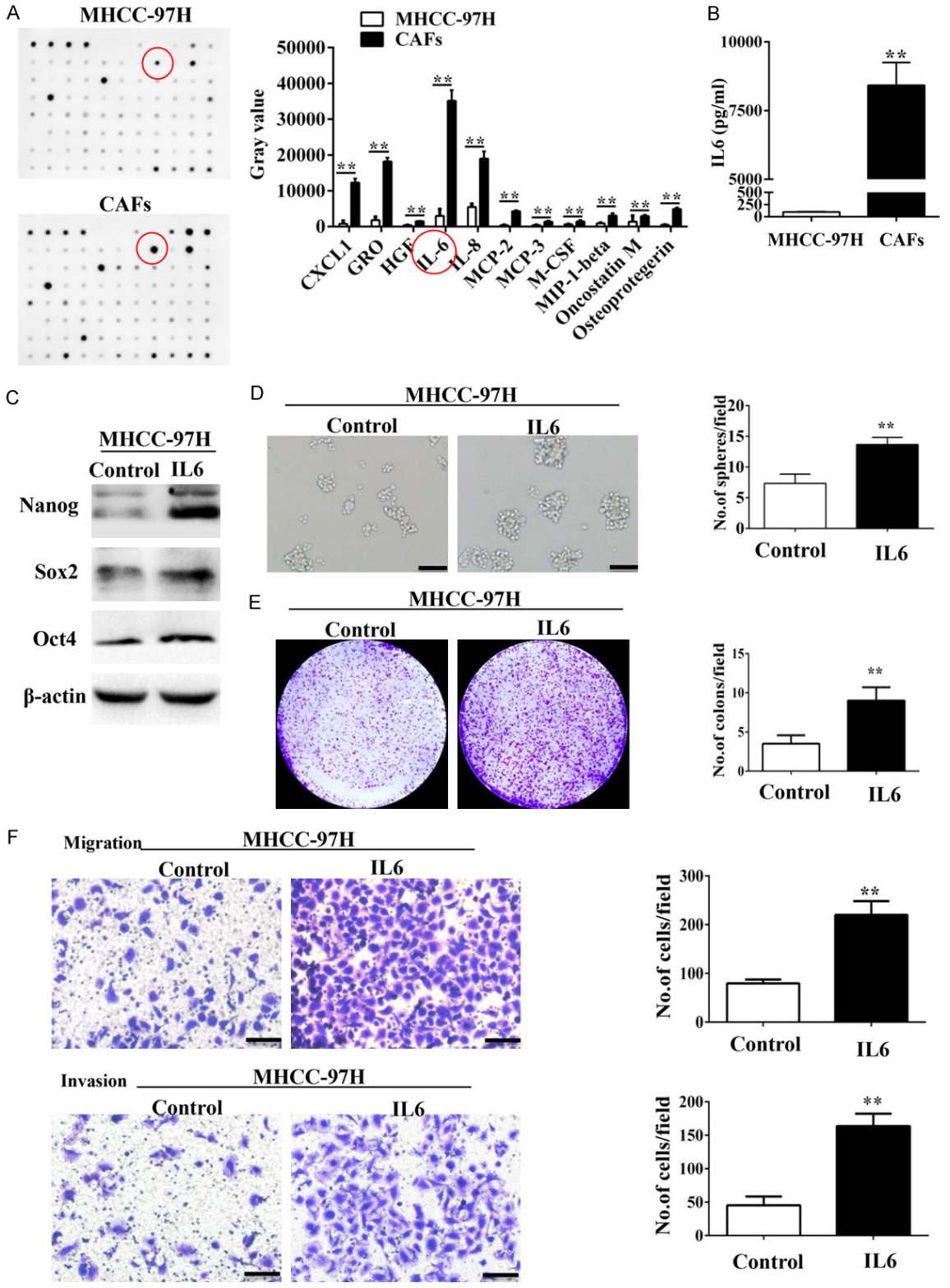

Figure 3. IL-6 secreted from CAFs enhances the stem cell-like properties of HCC cells. (A) Cytokine profiles of the CM from MHCC-97H cells and MHCC-97H-stimulated CAFs were screened using the RayBio human cytokine antibody array. IL-6 was the most significantly secreted cytokine from CAFs. (B) There was dramatically more soluble IL-6 in the CM from MHCC-97H-stimulated CAFs compared with that of MHCC-97H cells as assessed by ELISA assay. (C) Nanog, Sox2, and Oct4 were overexpressed in MHCC-97H cells treated with IL6. (D-F) IL-6 enhanced the sphere-forming (D), colony-forming (E), and migration and invasion (F) abilities of MHCC-97H cells. Scale bar, 100 μm. Data are shown as the means ± SD from at least three independent experiments. (*P < 0.05, **P < 0.01).

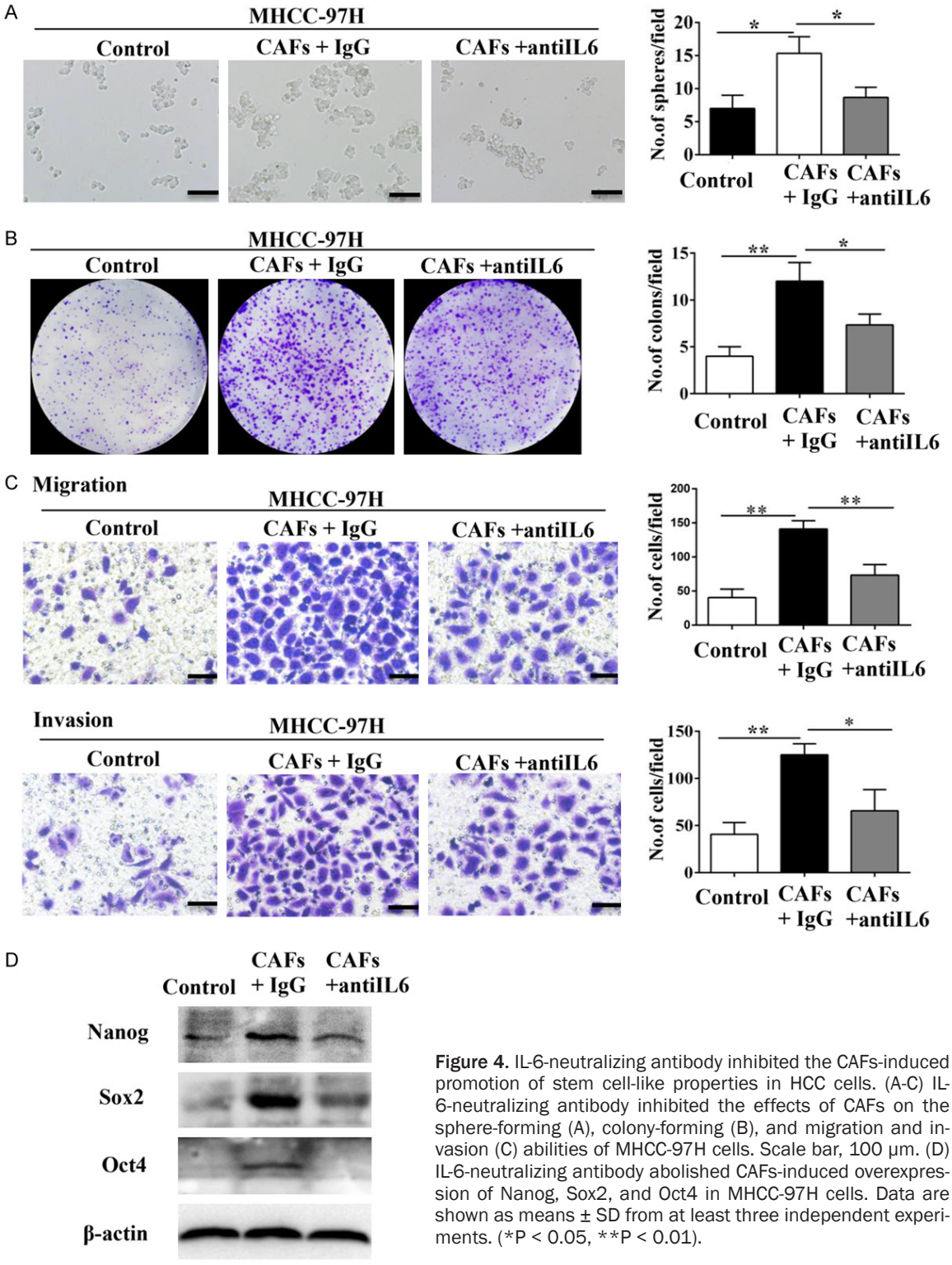

Figure 4. IL-6-neutralizing antibody inhibited the CAFs-induced promotion of stem cell-like properties in HCC cells. (A-C) IL-6-neutralizing antibody inhibited the effects of CAFs on the sphere-forming (A), colony-forming (B), and migration and invasion (C) abilities of MHCC-97H cells. Scale bar, 100 μm. (D) IL-6-neutralizing antibody abolished CAFs-induced overexpression of Nanog, Sox2, and Oct4 in MHCC-97H cells. Data are shown as means ± SD from at least three independent experiments. (*P < 0.05, **P < 0.01).

(CAFs) than peritumoral fibroblasts (PTFs) by western blotting and immunofluorescence (Figure S1B and S1C). In addition, the established CAFs showed negative expression for the endothelial marker CD31 and macrophage markers CD68 (Figure S2). These data were consistent with previous studies [8, 15, 26].

CSCs are characterized by stem cell-like properties such as self-renewal, proliferation, meta-

stasis and tumor initiation [2, 21, 27, 28]. Therefore, we investigated if CAFs regulate stem cell-like properties of HCC cells. To determine whether CAFs could regulate the self-renewal of HCC cells, MHCC-97H and HLE cells were subjected to a sphere formation assay by supplementation with either DMEM or the conditional medium (CM) of CAFs. When compared to HCC cells incubated with DMEM, a greater number of larger spheres were observed in HCC cells incubated with the CM of CAFs (**Figure 1A**). Colony formation assay further showed that MHCC-97H and HLE cells co-cultured with CAFs were able to produce a greater number of larger colonies compared to controls, indicating their effect on HCC proliferation (**Figure 1B**). In addition, Matrigel invasion and Transwell migration assays showed CAFs enhanced the migration and invasion abilities of MHCC-97H and HLE cells, highlighting their role in promoting HCC metastasis (**Figure 1C** and **1D**).

We further evaluated the expression of Nanog, Sox2 and Oct4, which are associated with induction and maintenance of CSCs [2]. We observed higher Nanog, Sox2 and Oct4 mRNA and protein expression in MHCC-97H and HLE cells co-cultured with CAFs than in controls (**Figure 1E** and **1F**). These data showed that CAFs induced stem cell-like properties in HCC cell lines.

Next, we examined if CAFs promoted in vivo tumorigenesis by subcutaneously injecting MHCC-97H (**Figure 2A**) or PLC/PRF/5 (**Figure 2B**) cells into NOD/SCID mice with or without CAFs in a 1:1 ratio. Mice injected with MHCC-97H and PLC/PRF/5 cells in combination with CAFs generated 3- and 5-fold higher mean tumor volume than control mice. These data were confirmed by H&E staining (**Figures 2**, S3).

IL-6 secreted by CAFs promotes stem cell-like properties in HCC cells

Cytokines produced by CAFs play important roles in modulating HCC progression [8, 11, 12, 15]. Therefore, we generated cytokine profiles of conditional media (CM) from MHCC-97H cells and MHCC-97H cells-stimulated CAFs with a Human Cytokine Array that screens 82 cytokines. Our data showed that CAFs secreted high amounts of IL-6 (**Figure 3A**). ELISA assay also showed that MHCC-97H cells-stimulated CAFs secreted high amounts of IL-6 than MHCC-97H cells alone (8392 pg/ml vs. 96 pg/ml; **Figure 3B**).

A recent study showed that IL-6 from tumor-associated macrophages (TAMs) promoted stem cell-like properties of HCC cells [29]. To test this hypothesis, we examined the effect of exogenous IL-6 on expression of Nanog, Sox2, and Oct4, which are three transcriptional factors that maintain stemness. Western blot analysis demonstrated that IL-6 up-regulated Nanog, Sox2, and Oct4 protein levels in MHCC-97H cells (**Figure 3C**). Further, IL-6 increased sphere and colony formation as well as migration and invasiveness of MHCC-97H cells (**Figure 3D-F**). Moreover, incubation with IL-6-neutralizing antibody inhibited up-regulation of Nanog, Sox2, and Oct4 in MHCC-97H cells (**Figure 4D**). The IL-6-neutralizing antibody also inhibited sphere and colony formation as well as migration and invasiveness of MHCC-97H cells co-cultured with CAFs (**Figure 4A-C**). These data suggested that IL-6 produced by CAFs induced stem cell-like properties in HCC cell lines.

IL-6 promotes stem cell-like properties of HCC cells through Notch signaling

Previous studies have revealed that cytokines initiate the embryonic signaling pathways, such as Notch, Wnt/β-catenin, and Hedgehog, contributing to CSC self-renewal and proliferation [12, 15, 17]. To investigate this hypothesis, we examined the activation of the Notch, Wnt/β-catenin and Hedgehog signaling pathways in MHCC-97H cells co-cultured with CAFs. We observed that only Notch signaling pathway components (Notch1 and Hes1) were the most significantly up-regulated proteins in MHCC-97H cells co-cultured with CAFs. (**Figure 5A** and **5B**). The similar observation was mimicked by treating MHCC-97H cells with IL-6. Moreover, IL-6-neutralizing antibody was able to block the effect of CAFs on activating Notch pathway in MHCC-97H cells (**Figure 5C**).

To determine the role of Notch1 in HCC progression, we performed lentivirus-based shRNA knockdown of Notch1 (shNOTCH1) in MHCC-97H cells (**Figure 5D**). Notch1 knockdown MHCC-97H cells co-cultured with CAFs or IL-6 showed decreased sphere and colony formation as well as migration and invasiveness than their corresponding controls (**Figure 5E-G**).

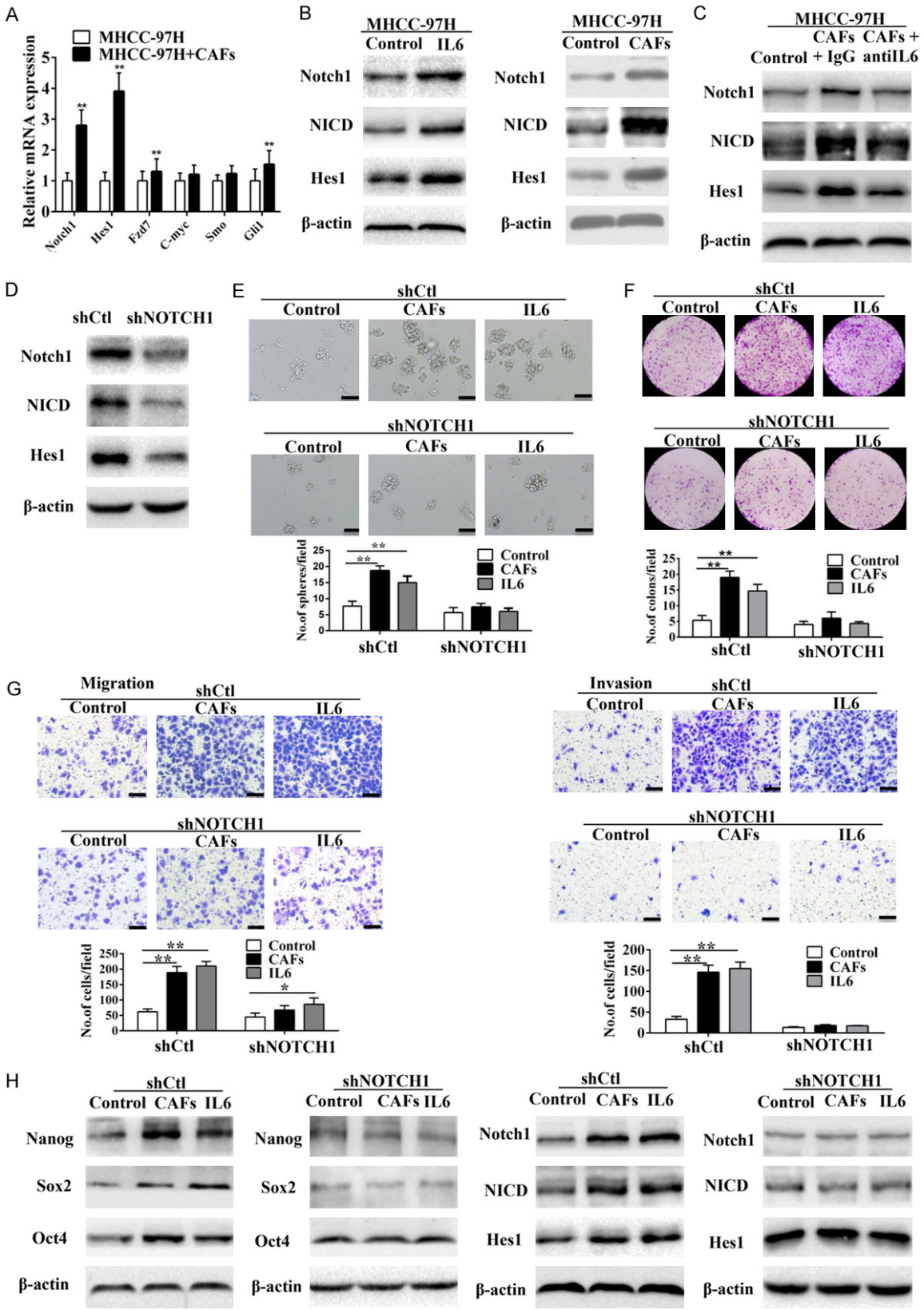

Figure 5. Notch signaling is required for IL6-induced enhancement of stem cell-like properties in HCC cells in vitro. (A) Expression levels of Notch, Hedgehog, and Wnt/β-catenin signaling components in MHCC-97H cells co-cultured with CAFs were detected by RT-PCR. (B) According to western blot analysis, Notch signaling was up-regulated in

MHCC-97H cells and HLE cells co-cultured with CAFs. (C) IL-6-neutralizing antibody abolished CAFs-induced overexpression of Notch signaling components (Notch1, NICD, and Hes1) in MHCC-97H cells. (D) Knockdown of Notch1 by shNOTCH1. (E and G) IL6- or CAFs-induced sphere-forming (E), colony-forming (F), and migration and invasion (G) abilities of MHCC-97H cells were reduced when Notch signaling was blocked by shNOTCH1. Scale bar, 100 μm. (H) Knockdown of Notch1 abolished IL6- or CAFs-induced overexpression of Notch signaling components (Notch1, NICD, and Hes1) and stemness-associated genes (Nanog, Sox2, and Oct4) in MHCC-97H cells. Data are shown as means ± SD from at least three independent experiments. (*P < 0.05, **P < 0.01).

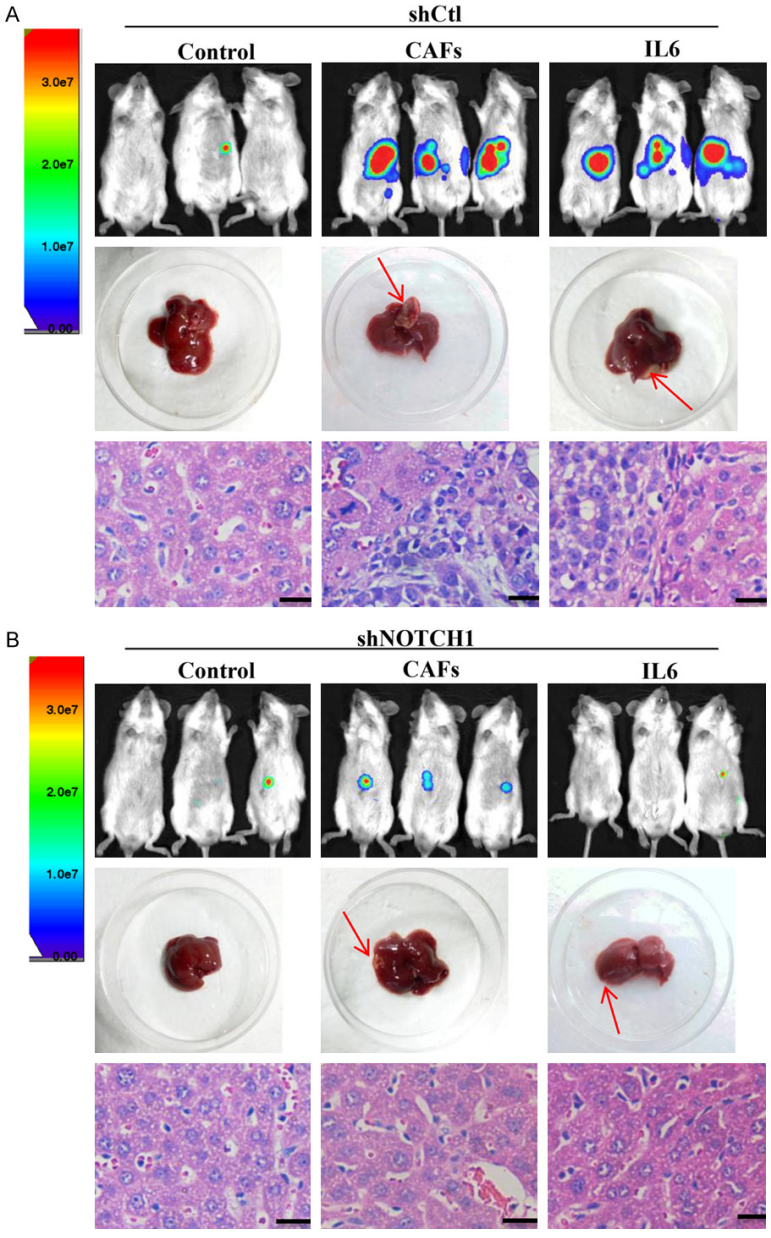

Figure 6. Notch signaling is required for IL6-induced enhancement of stem cell-like properties of HCC cells in vivo. Luciferase-labelled MHCC-97H cells transfected with lentiviral plasmid containing Notch1-shRNA (shNOTCH1) (A) or vector control (shCtl) (B) were injected into the livers of NOD/SCID mice either alone, with CAFs, or with IL-6. In the shCtl group, MHCC-97H cells treated with IL-6 or CAFs formed a greater number of larger tumors, and this effect was abolished upon Notch1 knockdown. Red arrow indicates the site of tumor formation for MHCC-97H cells in the livers of NOD/SCID mice. Paraffin-embedded tissues of xenotransplanted tumors were processed for H&E staining. Scale bar, 50 μm.

Moreover, knockdown of Notch1 abolished induction of Notch signaling components (Notch1, NICD, and Hes1) and stemness-associated genes (Nanog, Sox2, and Oct4) in MHCC-97H cells when co-cultured with CAFs or IL-6 (**Figure 5H**). Consistently, Notch pathway inhibited by RO4929097, a γ-secretase inhibitor [21], could also hinder CAFs induced stemness of MHCC-97H cells (Figure S4). Hence, CAFs induced stemness in HCC cells by activating Notch signaling.

Next, we injected Notch1 knockdown (shNOTCH1) or control (shCtl) MHCC-97H cells into the livers of NOD/SCID mice with or without CAFs or IL-6. The control MHCC-97H cells formed larger liver tumors in the presence with IL-6 or CAFs than Notch1 knockdown MHCC-97H cells (**Figure 6A** and **6B**). Collectively, these results suggest that IL-6 secreted from CAFs promotes the HCC progression by inducing Notch signaling.

IL-6 induces Notch signaling via STAT3 phosphorylation

Stemness of breast cancer cells is regulated by the crosstalk between IL6/STAT3 and Notch signaling, which is mediated by myeloid-derived suppressor cells (MDSCs) [30]. In this study, we found increased phospho-STAT3 (Tyr705) levels in MHCC-97H

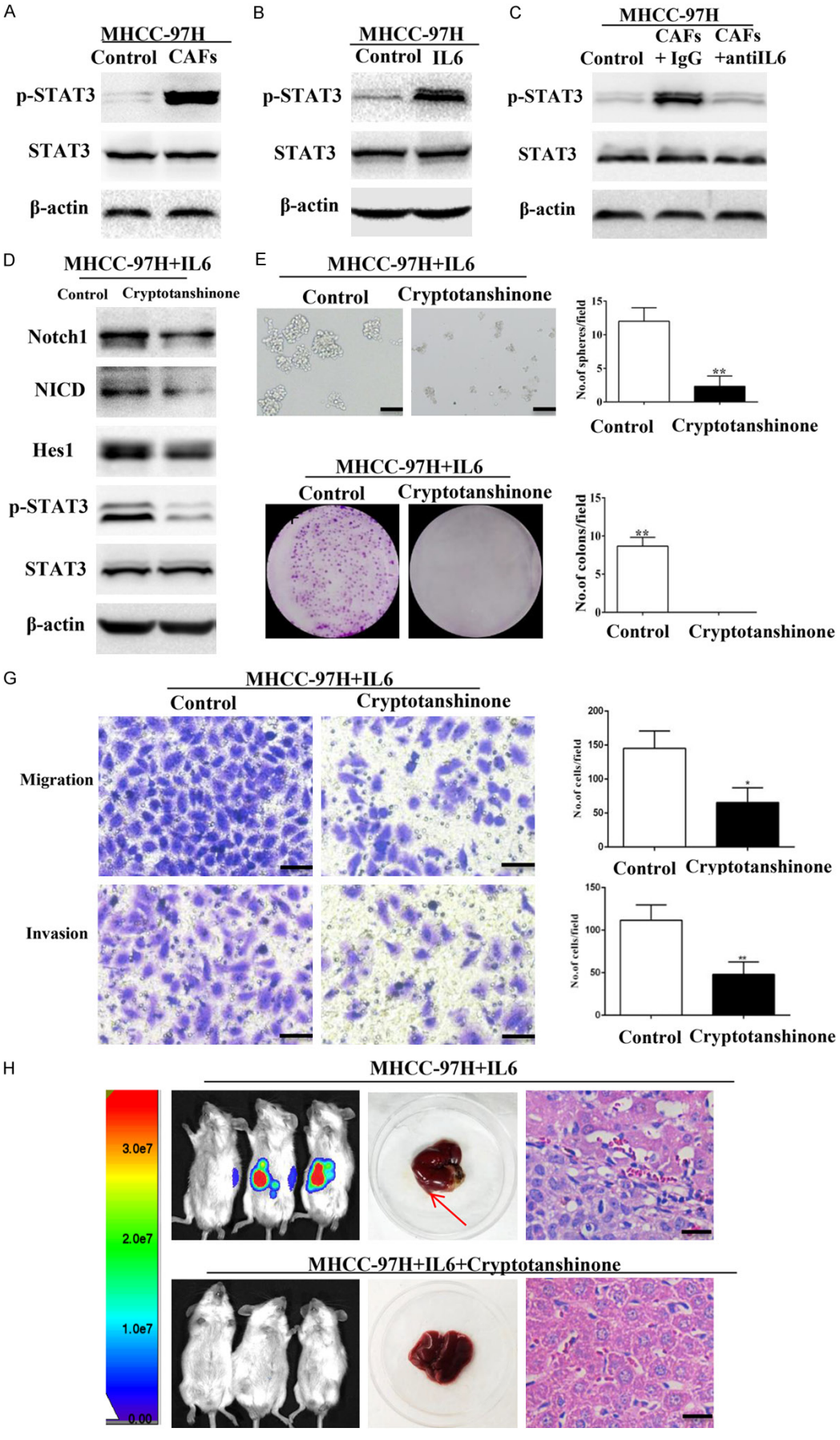
A
MHCC-97H
Control CAFs
p-STAT3
STAT3
β-actin
B
MHCC-97H
Control IL6
p-STAT3
STAT3
β-actin
C
MHCC-97H
Control CAFs + IgG CAFs +antiIL6
p-STAT3
STAT3
β-actin
D
MHCC-97H+IL6
Control Cryptotanshinone
Notch1
NICD
Hes1
p-STAT3
STAT3
β-actin
E
MHCC-97H+IL6
Control Cryptotanshinone
No.of spheres/field
Control Cryptotanshinone
MHCC-97H+IL6
Control Cryptotanshinone
No.of colons/field
Control Cryptotanshinone
G
MHCC-97H+IL6
Control Cryptotanshinone
Migration
Invasion
No.of cells/field
Control Cryptotanshinone
No.of cells/field
Control Cryptotanshinone
H
MHCC-97H+IL6
3.0e7
2.0e7
1.0e7
0.00
MHCC-97H+IL6+Cryptotanshinone

Figure 7. IL-6 induces the activation of Notch signaling via STAT3 Tyr705 phosphorylation. (A, B) Phospho-STAT3 (Tyr705) was elevated in MHCC-97H cells treated with CAFs (A) or IL-6 (B). (C) IL-6-neutralizing antibody abolished CAFs-induced overexpression of Phospho-STAT3 (Tyr705) in MHCC-97H cells. (D) Cryptotanshinone suppressed the expression of phospho-STAT3 and Notch signaling components (Notch1, NICD, and Hes1) in MHCC-97H cells treated with IL-6. (E, G) IL-6-induced sphere-forming (E), colony-forming (F), and migration and invasion (G) abilities of MHCC-97H cells decreased when STAT3 Tyr705 phosphorylation was inhibited by cryptotanshinone. Scale bar, 100 μm. (H) MHCC-97H cells treated with IL-6 in the presence or absence of cryptotanshinone were injected into the livers of NOD/SCID mice. Inhibition of STAT3 Tyr705 phosphorylation abolished the effect of IL-6. Paraffin-embedded tissues of xenotransplanted tumours were processed for H&E staining. Scale bar, 50 μm. Red arrow indicates the site of tumor formation of MHCC-97H cells in the livers of NOD/SCID mice. Data are shown as means ± SD from at least three independent experiments. (*P < 0.05, **P < 0.01).

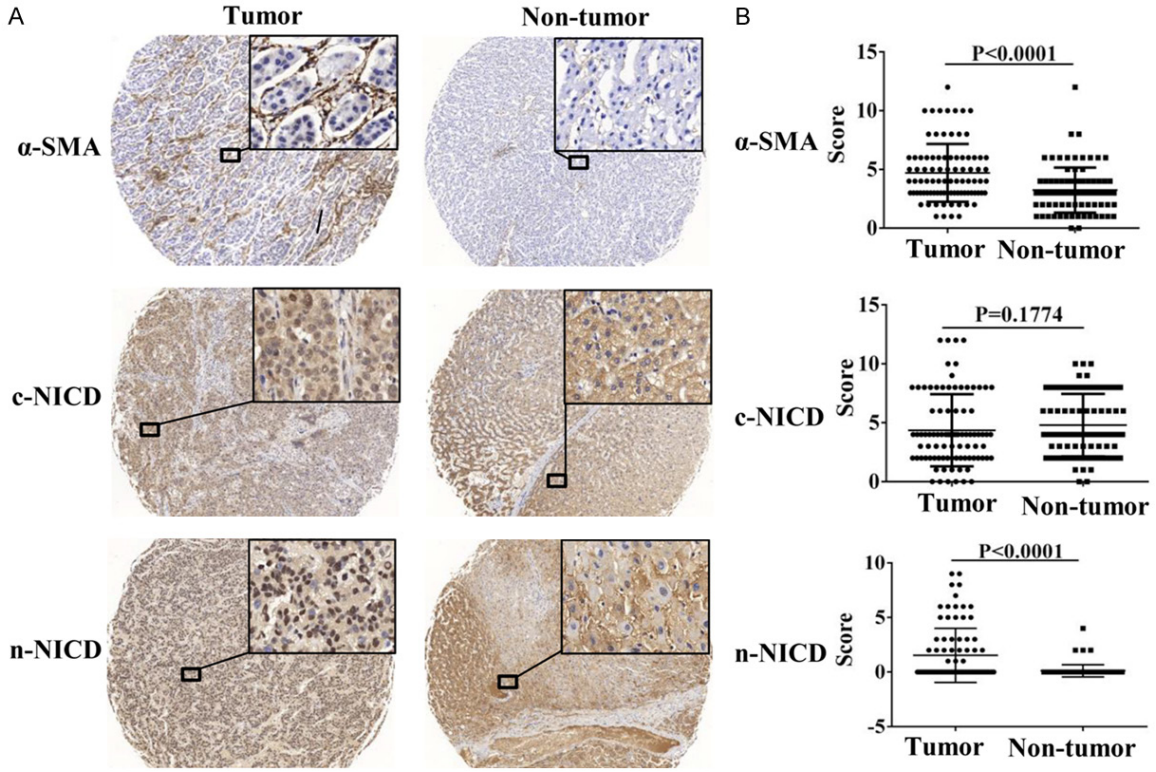

Figure 8. NICD and α-SMA expression levels are up-regulated in HCC tissues. A. NICD was expressed in the nuclei and cytoplasm of tumor cells, and α-SMA was expressed in the cytoplasm of CAFs. The expression levels of nuclear NICD and α-SMA in tumors were markedly higher than those in adjacent non-tumor tissues. Magnifications of all images are ×40 (left) and ×400 (right). B. Analysis of expression levels of NICD and α-SMA in tumor and adjacent non-tumor tissues by paired t-test.

cells treated with IL-6 or CAFs (**Figure 7A-C**). This suggested that STAT3 phosphorylation may mediate activation of Notch signaling in HCC cells. We tested this hypothesis by treating MHCC-97H cells with IL-6 in the presence or absence of Cryptotanshinone, an inhibitor of STAT3 Tyr705 phosphorylation [31]. Cryptotanshinone decreased phospho-STAT3 levels and expression of Notch signaling-associated components (Notch1, NICD, and Hes1) in MHCC-97H cells treated with IL-6 (**Figure 7D**). Furthermore, inhibition of STAT3 phosphorylation decreased sphere and colony formation as well as migration and invasion of MHCC-97H cells treated with IL-6 (**Figure 7E-G**). Cryptotanshinone also reduced liver tumor growth in NOD/SCID mice injected with MHCC-97H cells and IL-6 (**Figure 7H**). Consistently, STAT3 phosphorylation inhibited by Stattic, an inhibitor of STAT3 Tyr705 phosphorylation [32], could also hinder IL6 induced stemness and activation of Notch signaling in MHCC-97H cells (Figure S5).

Table 1. The correlation between the expression of nNICD and clinical-pathological features in HCC patients

Clinical-Pathological Variables	High nNICD N=15	Low nNICD N=73	*p* Value
Venous Infiltration	-	-	
Absence	6	66	
Presence	9	7	P<0.001**
Serum AFP Level			
Low (≤ 400 ng/ml)	6	39	
High (> 400 ng/ml)	9	34	P=0.343
Age			
Young (≤ median, 50)	10	43	
Old (> median, 50)	5	30	P=0.576
Differentiation Status			
Well differentiated	2	17	
Moderately to poorly differentiated	13	56	P=0.508
Tumor Size			
Small (≤ 5 cm)	4	18	
Large (> 5 cm)	11	55	P=1
HBV Association			
Negative	0	16	
Positive	15	57	P=0.063
Lymph node metastasis			
Absence	9	68	
Presence	6	5	P=0.003**
Sex			
Male	15	63	
Female	0	10	P=0.2

*P < 0.05, Signiicant difference, **P < 0.01, Signiicant difference (χ^2 test and Fisher's exact test).

These data suggest that STAT3 Tyr705 phosphorylation may mediate IL-6 and Notch signaling.

High nuclear NICD expression in HCC cells correlates with poor prognosis in HCC patients

We retrospectively evaluated the expression of α-SMA and NICD in 88 matched human HCC and adjacent normal liver tissue specimens. Immunohistochemical staining showed that the activated fibroblast marker, α-SMA was cytoplasmic and overexpressed in tumor tissues. NICD was expressed in both the cytoplasm and the nuclei of tumor and peri-tumor tissues. When accounting for cytoplasmic NICD (cNICD) and nuclear NICD (nNICD), respectively, we observed only nNICD but not cNICD was overexpressed in tumor tissues compared to those in adjacent non-tumor tissues (**Figure 8A** and **8B**). There was a strong correlation between the high α-SMA expression in CAFs and high expression of nNICD in HCC cells (Table S1). High expression of nNICD in HCC tissues strongly correlated with venous infiltration (P < 0.0001) and lymph node metastasis (P=0.003; **Table 1**). Hence, high nNICD expression indicated poor prognosis in HCC patients.

Discussion

Although previous studies have shown that CAFs promote HCC progression by enhancing tumor cell proliferation and invasion, the underlying mechanisms are not known. In this study, we found that CAFs induce expression of stemness-associated transcription factors such as Nanog, Sox2 and Oct4 in HCC cell lines. CAFs modulated stem cell-like properties of HCC cells by secreting IL-6, which activated Notch signaling via STAT3 phosphorylation. Moreover, high nuclear expression of NICD in tumor cells correlated with poor prognosis of HCC patients. Therefore, we postulate that CAFs promote HCC progression by modulating IL-6/STAT3/Notch signaling.

It has been well recognized that HCC is driven and maintained by CSCs that display stem cell-like properties [2, 33]. Recent studies marked the tumor cell plasticity with a phenomenon whereby a non-CSC spontaneously dedifferentiates into a CSC in the tumor microenvironment [4, 5, 30]. CAFs represent one of the major cell types found in a tumor microenvironment and are associated with several malignancies [6]. Most HCC cases are related to liver cirrhosis, which is accompanied by enrichment of activated fibroblasts due to chronic inflammation that eventually transform into CAFs [9, 10]. Therefore, CAFs are probably involved in dedifferentiation of HCC cells. Previous studies

have shown that CAF promote stemness by secreting cytokines such as IGF-II in lung cancer [4] and CCL2 in breast cancer [12]. Moreover, CAFs regulate tumor-initiating cell plasticity in HCC through HGF [8]. In this study, we demonstrate that IL-6 was the most significantly secreted cytokine by CAFs related to HCC.

IL-6 plays an important role in tumor development as well as the conversion of non-CSC into CSC [29, 34, 35]. We demonstrated that the stem cell-like properties of HCC cells were dependent on IL-6 produced by CAFs (**Figures 3**, **4**). The IL-6/Notch signaling cascade regulated the stem cell-like properties of HCC cells and these effects were inhibited by the IL-6 neutralizing antibody or shRNA knockdown of Notch1 (**Figures 4**, **5**).

Notch signaling plays critical roles in the development of cancer and self-renewal of CSC [17, 36-38]. In particular, Notch signaling regulates the stem cell-like properties of HCC cells [21, 39]. However, the consequence of the interaction between IL-6 and Notch signaling in HCC is not documented. In a recent study, crosstalk between MDSCs and CSCs via IL-6/STAT3 and Notch signaling was essential for breast cancer progression [30]. STAT3 signaling plays a critical role in the progress of HCC [11, 29]. IL-6/STAT3 signaling regulates CSC characteristics in colorectal [40], and gastric [41] cancers. Therefore, we investigated if STAT3 activation linked IL-6 and Notch signaling in HCC cells. We found that IL-6 released by CAFs induced phosphorylation of STAT3, which activated Notch signaling. By using cryptotanshinone to block STAT3 Tyr705 phosphorylation, we found that STAT3 Tyr705 phosphorylation may mediate IL-6 and Notch signaling. (**Figure 7**). Overall, these data suggest that the IL-6/STAT3/Notch signaling cascade may play a critical role in promoting the stem cell-like characteristics of HCC cells.

Our study demonstrates that IL-6 enhances stem cell-like properties of HCC cells. This is supported by experiments with anti-IL6 antibody that partially blocks these effects. However, the role of other cytokines secreted by CAFs cannot be ruled out. Previous studies have shown that CAFs play important roles in the development of HCC through HGF [8], CCL2, CCL5, CCL7, CXCL16 [15], TGF-β, SDF1 [16], and exosomes [42]. Since CAFs secrete a large number of cytokines that modulate HCC progression, further studies are needed to clarify the role of other CAFs-related cytokines in the regulation of stem cell-like characteristics of HCC cells. Our data also demonstrates that Tyr705 phosphorylation of STAT3 may activate Notch signaling. Interestingly, Notch4/STAT3 crosstalk is important for EMT in breast cancer [43]. In addition, a recent study indicates that CAF-mediated maintenance of the liver CSC state, and the enhanced liver CSC tumorigenicity were abolished after knockdown of Notch3 [44]. We propose to further investigate the role of STAT3 activation and Notch signaling in HCC progression.

In summary, our results show that CAFs enhance stem cell-like characteristics of HCC cells via the IL-6/STAT3/Notch signaling cascade. This study also highlights the therapeutic potential of targeting IL-6/STAT3/Notch signaling cascade and CAFs in HCC.

Acknowledgements

This work was supported by grants from the National Natural Science Foundation of China (81172063 and 81372352).

Disclosure of conflict of interest

None.

Abbreviations

CSCs, Cancer stem cells; HCC, hepatocellular carcinoma; CAFs, cancer-associated fibroblasts; PTFs, peri-tumor fibroblasts; α-SMA, alpha-smooth muscle actin; IL-6, interleukin 6; NICD, Notch intracellular domain; STAT3, signal transducer and activator of transcription 3; FAP, fibroblast activation protein; MDSCs, myeloid-derived suppressor cells; cNICD, cytoplasmic NICD; nNICD, nuclear NICD.

Address correspondence to: Dr. Bin Cheng, Department of Gastroenterology and Hepatology, Tongji Hospital, Tongji Medical College, Huazhong University of Science and Technology, Wuhan 430030, PR China. Tel: +86-27 83663595; Fax: +86-27 83663585; E-mail: b.cheng@tjh.tjmu.edu.cn

References

[1] Forner A, Llovet JM and Bruix J. Hepatocellular carcinoma. Lancet 2012; 379: 1245-1255.

[2] Lee TK, Castilho A, Cheung VC, Tang KH, Ma S and Ng IO. CD24(+) liver tumor-initiating cells drive self-renewal and tumor initiation through STAT3-mediated NANOG regulation. Cell Stem Cell 2011; 9: 50-63.

[3] Yang ZF, Ho DW, Ng MN, Lau CK, Yu WC, Ngai P, Chu PW, Lam CT, Poon RT, Fan ST. Significance of CD90+ cancer stem cells in human liver cancer. Cancer Cell 2008; 13: 153-166.

[4] Chen WJ, Ho CC, Chang YL, Chen HY, Lin CA, Ling TY, Yu SL, Yuan SS, Chen YJ, Lin CY, Pan SH, Chou HY, Chen YJ, Chang GC, Chu WC, Lee YM, Lee JY, Lee PJ, Li KC, Chen HW and Yang PC. Cancer-associated fibroblasts regulate the plasticity of lung cancer stemness via paracrine signalling. Nat Commun 2014; 5: 3472.

[5] Yan GN, Yang L, Lv YF, Shi Y, Shen LL, Yao XH, Guo QN, Zhang P, Cui YH, Zhang X, Bian XW and Guo DY. Endothelial cells promote stem-like phenotype of glioma cells through activating the Hedgehog pathway. J Pathol 2014; 234: 11-22.

[6] Hanahan D and Coussens LM. Accessories to the crime: functions of cells recruited to the tumor microenvironment. Cancer Cell 2012; 21: 309-322.

[7] Kise K, Kinugasa-Katayama Y and Takakura N. Tumor microenvironment for cancer stem cells. Adv Drug Deliv Rev 2016; 99: 197-205.

[8] Lau EY, Lo J, Cheng BY, Ma MK, Lee JM, Ng JK, Chai S, Lin CH, Tsang SY, Ma S, Ng IO and Lee TK. Cancer-associated fibroblasts regulate tumor-initiating cell plasticity in hepatocellular carcinoma through c-Met/FRA1/HEY1 signaling. Cell Rep 2016; 15: 1175-1189.

[9] Luedde T and Schwabe RF. NF-kappaB in the liver–linking injury, fibrosis and hepatocellular carcinoma. Nat Rev Gastroenterol Hepatol 2011; 8: 108-118.

[10] Affo S, Yu LX and Schwabe RF. The role of cancer-associated fibroblasts and fibrosis in liver cancer. Annu Rev Pathol 2017; 12: 153-186.

[11] Zheng X, Xu M, Yao B, Wang C, Jia Y and Liu Q. IL-6/STAT3 axis initiated CAFs via up-regulating TIMP-1 which was attenuated by acetylation of STAT3 induced by PCAF in HCC microenvironment. Cell Signal 2016; 28: 1314-1324.

[12] Tsuyada A, Chow A, Wu J, Somlo G, Chu P, Loera S, Luu T, Li AX, Wu X, Ye W, Chen S, Zhou W, Yu Y, Wang YZ, Ren X, Li H, Scherle P, Kuroki Y and Wang SE. CCL2 mediates cross-talk between cancer cells and stromal fibroblasts that regulates breast cancer stem cells. Cancer Res 2012; 72: 2768-2779.

[13] Hasegawa T, Yashiro M, Nishii T, Matsuoka J, Fuyuhiro Y, Morisaki T, Fukuoka T, Shimizu K, Shimizu T, Miwa A and Hirakawa K. Cancer-associated fibroblasts might sustain the stemness of scirrhous gastric cancer cells via transforming growth factor-beta signaling. Int J Cancer 2014; 134: 1785-1795.

[14] Wu X, Tao P, Zhou Q, Li J, Yu Z, Wang X, Li J, Li C, Yan M, Zhu Z, Liu B, Su L. IL-6 secreted by cancer-associated fibroblasts promotes epithelial-mesenchymal transition and metastasis of gastric cancer via JAK2STAT3 signaling pathway. Oncotarget 2017; 8: 20741-20750.

[15] Liu J, Chen S, Wang W, Ning BF, Chen F, Shen W, Ding J, Chen W, Xie WF and Zhang X. Cancer-associated fibroblasts promote hepatocellular carcinoma metastasis through chemokine-activated hedgehog and TGF-beta pathways. Cancer Lett 2016; 379: 49-59.

[16] Yang J, Lu Y, Lin YY, Zheng ZY, Fang JH, He S and Zhuang SM. Vascular mimicry formation is promoted by paracrine TGF-beta and SDF1 of cancer-associated fibroblasts and inhibited by miR-101 in hepatocellular carcinoma. Cancer Lett 2016; 383: 18-27.

[17] Takebe N, Harris PJ, Warren RQ and Ivy SP. Targeting cancer stem cells by inhibiting Wnt, Notch, and Hedgehog pathways. Nat Rev Clin Oncol 2011; 8: 97-106.

[18] Pupo M, Pisano A, Abonante S, Maggiolini M and Musti AM. GPER activates Notch signaling in breast cancer cells and cancer-associated fibroblasts (CAFs). Int J Biochem Cell Biol 2014; 46: 56-67.

[19] Fan X, Khaki L, Zhu TS, Soules ME, Talsma CE, Gul N, Koh C, Zhang J, Li YM, Maciaczyk J, Nikkhah G, Dimeco F, Piccirillo S, Vescovi AL and Eberhart CG. NOTCH pathway blockade depletes CD133-positive glioblastoma cells and inhibits growth of tumor neurospheres and xenografts. Stem Cells 2010; 28: 5-16.

[20] Winton DJ. miR-34a sets the “sweet spot” for notch in colorectal cancer stem cells. Cell Stem Cell 2013; 12: 499-501.

[21] Luo J, Wang P, Wang RH, Wang JL, Liu M, Xiong S, Li YW, Cheng B. The Notch pathway promotes the cancer stem cell characteristics of CD90+ cells in hepatocellular carcinoma. Oncotarget 2016; 7: 9525-37.

[22] Fan ST, Lo CM, Liu CL, Lam CM, Yuen WK, Yeung C, Wong J. Hepatectomy for hepatocellular carcinoma: toward zero hospital deaths. Ann Surg 1999; 229: 322-30.

[23] Zeng Z, Ren J, O’Neil M, Zhao J, Bridges B, Cox J, Abdulkarim B, Schmitt TM, Kumer SC and Weinman SA. Impact of stem cell marker expression on recurrence of TACE-treated hepatocellular carcinoma post liver transplantation. BMC Cancer 2012; 12: 584.

[24] Shan J, Shen J, Liu L, Xia F, Xu C, Duan G, Xu Y, Ma Q, Yang Z, Zhang Q, Ma L, Liu J, Xu S, Yan X,

Bie P, Cui Y, Bian XW and Qian C. Nanog regulates self-renewal of cancer stem cells through the insulin-like growth factor pathway in human hepatocellular carcinoma. Hepatology 2012; 56: 1004-1014.
[25] Wang F, Zhou H, Xia X, Sun Q, Wang Y and Cheng B. Activated Notch signaling is required for hepatitis B virus X protein to promote proliferation and survival of human hepatic cells. Cancer Lett 2010; 298: 64-73.
[26] Richards KE, Zeleniak AE, Fishel ML, Wu J, Littlepage LE and Hill R. Cancer-associated fibroblast exosomes regulate survival and proliferation of pancreatic cancer cells. Oncogene 2017; 36: 1770-1778.
[27] Todaro M, Gaggianesi M, Catalano V, Benfante A, Iovino F, Biffoni M, Apuzzo T, Sperduti I, Volpe S, Cocorullo G, Gulotta G, Dieli F, De Maria R and Stassi G. CD44v6 is a marker of constitutive and reprogrammed cancer stem cells driving colon cancer metastasis. Cell Stem Cell 2014; 14: 342-356.
[28] Manrique I, Nguewa P, Bleau AM, Nistal-Villan E, Lopez I, Villalba M, Gil-Bazo I and Calvo A. The inhibitor of differentiation isoform Id1b, generated by alternative splicing, maintains cell quiescence and confers self-renewal and cancer stem cell-like properties. Cancer Lett 2015; 356: 899-909.
[29] Wan S, Zhao E, Kryczek I, Vatan L, Sadovskaya A, Ludema G, Simeone DM, Zou W and Welling TH. Tumor-associated macrophages produce interleukin 6 and signal via STAT3 to promote expansion of human hepatocellular carcinoma stem cells. Gastroenterology 2014; 147: 1393-1404.
[30] Peng D, Tanikawa T, Li W, Zhao L, Vatan L, Szeliga W, Wan S, Wei S, Wang Y, Liu Y, Staroslawska E, Szubstarski F, Rolinski J, Grywalska E, Stanislawek A, Polkowski W, Kurylcio A, Kleer C, Chang AE, Wicha M, Sabel M, Zou W and Kryczek I. Myeloid-derived suppressor cells endow stem-like qualities to breast cancer cells through IL6/STAT3 and NO/NOTCH cross-talk signaling. Cancer Res 2016; 76: 3156-3165.
[31] Shin DS, Kim HN, Shin KD, Yoon YJ, Kim SJ, Han DC and Kwon BM. Cryptotanshinone inhibits constitutive signal transducer and activator of transcription 3 function through blocking the dimerization in DU145 prostate cancer cells. Cancer Res 2009; 69: 193-202.
[32] Schust J, Sperl B, Hollis A, Mayer TU and Berg T. Stattic: a small-molecule inhibitor of STAT3 activation and dimerization. Chem Biol 2006; 13: 1235-1242.
[33] Yang ZF, Ho DW, Ng MN, Lau CK, Yu WC, Ngai P, Chu PW, Lam CT, Poon RT and Fan ST. Significance of CD90+ cancer stem cells in human liver cancer. Cancer Cell 2008; 13: 153-166.
[34] He G, Dhar D, Nakagawa H, Font-Burgada J, Ogata H, Jiang Y, Shalapour S, Seki E, Yost SE, Jepsen K, Frazer KA, Harismendy O, Hatziapostolou M, Iliopoulos D, Suetsugu A, Hoffman RM, Tateishi R, Koike K and Karin M. Identification of liver cancer progenitors whose malignant progression depends on autocrine IL-6 signaling. Cell 2013; 155: 384-396.
[35] Wang C, Sun H, Gao X, Ren N, Sheng Y, Wang Z, Zheng Y, Wei J, Zhang K, Yu X, Zhu Y, Luo Q, Yang L, Dong Q, Qin L. Interleukin-6 enhances cancer stemness and promotes metastasis of hepatocellular carcinoma via up-regulating osteopontin expression. Am J Cancer Res 2016; 6: 1873-1889.
[36] Gao J, Long B, Wang Z. Role of Notch signaling pathway in pancreatic cancer. Am J Cancer Res 2017; 7: 173-186.
[37] Zhang H, Zhang CF, Chen R. Zinc finger RNA-binding protein promotes non-small-cell carcinoma growth and tumor metastasis by targeting the Notch signaling pathway. Am J Cancer Res 2017; 7: 1804-1819.
[38] Zhu H, Bhaijee F, Ishaq N, Pepper DJ, Backus K, Brown AS, Zhou X, Miele L. Correlation of Notch1, pAKT and nuclear NF-κB expression in triple negative breast cancer. Am J Cancer Res 2013; 3: 230-9.
[39] Wang RH, Sun Q, Wang P, Liu M, Xiong S, Luo J, Huang H, Du Q, Geller DA, Cheng B. Notch and Wntβ-catenin signaling pathway play important roles in activating liver cancer stem cells. Oncotarget 2016; 7: 5754-68.
[40] Lin L, Fuchs J, Li C, Olson V, Bekaii-Saab T and Lin J. STAT3 signaling pathway is necessary for cell survival and tumorsphere forming capacity in ALDH(+)/CD133(+) stem cell-like human colon cancer cells. Biochem Biophys Res Commun 2011; 416: 246-251.
[41] Zhu Q, Zhang X, Zhang L, Li W, Wu H, Yuan X, Mao F, Wang M, Zhu W, Qian H and Xu W. The IL-6-STAT3 axis mediates a reciprocal crosstalk between cancer-derived mesenchymal stem cells and neutrophils to synergistically prompt gastric cancer progression. Cell Death Dis 2014; 5: e1295.
[42] Zhang Z, Li X, Sun W, Yue S, Yang J, Li J, Ma B, Wang J, Yang X, Pu M, Ruan B, Zhao G, Huang Q, Wang L, Tao K and Dou K. Loss of exosomal miR-320a from cancer-associated fibroblasts contributes to HCC proliferation and metastasis. Cancer Lett 2017; 397: 33-42.
[43] Bui QT, Im JH, Jeong SB, Kim YM, Lim SC, Kim B and Kang KW. Essential role of Notch4/STAT3 signaling in epithelial-mesenchymal transition of tamoxifen-resistant human breast cancer. Cancer Lett 2017; 390: 115-125.
[44] Liu C, Liu L, Chen X, Cheng J, Zhang H, Zhang C, Shan J, Shen J and Qian C. LSD1 stimulates cancer-associated fibrobasts to drive Notch3-dependent self-renewal of liver cancer stem-like cells. Cancer Res 2017; [Epub ahead of print].

Supplementary materials and methods

Sphere formation assay

To assay sphere formation efficiency, a single-cell suspension of HCC cells was created in serum-free DMEM/F12 medium (cat# 12400-024; GIBCO) with 20 ng/ml human recombinant epidermal growth factor (EGF; cat# PHG0311; GIBCO), 10 ng/ml human recombinant basic fibroblast growth factor (bFGF; cat# PHG0266; GIBCO), 100 IU/ml penicillin, 100 μg/ml streptomycin, 2% B27 supplement (cat# 17504-044; GIBCO), 1% N-2 supplement (cat# 17502-048; GIBCO), and 1% methyl cellulose (cat# M0262; Sigma-Aldrich, St. Louis, MO, USA) to prevent cell aggregation. Cells were subsequently seeded in ultra-low adherence 24-well plates (Corning, NY, USA; 200 viable cells per well) at a density of 10^4 cells/ml. Spheres containing over 100 cells were counted.

Quantitative RT-PCR

Total RNA was isolated from cancer cells according to the standard TRIzol (Takara, Tokyo, Japan) method. cDNA synthesis was performed using PrimeScript RT Master Mix (Takara) according to the manufacturer's instructions. Quantitative PCR was performed with SYBR Premix Ex Taq (cat# DRR081A; Takara) using an ABI StepOne Real-time Detection System. PCR reaction conditions for all assays were 94°C for 30 s followed by 40 cycles of 94°C for 5 s, 60°C for 30 s, and 72°C for 30 s. β-actin mRNA was used as an internal control. RT-PCR primers are presented in Table S3.

Invasion assay

Cell invasion was detected using Transwell chambers (8-μm pore size; Millipore, Billerica, MA, USA) with a Matrigel (BD Biosciences, San Jose, CA, USA) matrix. In brief, 3×10^4 cells were seeded on the upper chamber with serum-free DMEM. DMEM medium with 10% FBS was added to the lower chamber. After 24 h, HCC cells that invaded through the Matrigel-coated Transwell inserts were fixed in 95% ethanol and stained with a 4 g/l crystal violet solution. Photographs of three randomly selected fields of fixed cells were captured, and cells were counted. Each experiment was repeated three times.

Colony formation assay

Cells were seeded at a density of 3,000 cells per well in 6-well plates and allowed to grow for 10 days. Next, the colonies were fixed in 4% methanol and stained with a 4 g/l crystal violet solution. Colonies containing over 50 cells were counted.

Collection of CM

CAFs or HCC cells were seeded on 6-well plates at 1×10^5 cells per well. Culture medium was removed 72 h after cell seeding. Cells were washed twice with PBS, and 1 ml of serum-free medium was added per well. After 24 h of incubation at 37°C and 5% CO_2 atmosphere, the CM was collected and passed through a 0.2-mm membrane syringe filter to remove any cells and cell debris.

Human cytokine antibody array

The profiles of cytokine secreted by CAFs and MHCC-97H were detected with the culture supernatants of CAFs and MHCC-97H using a Human cytokine Array (RayBiotech AAH-CYT-5, Norcross, GA) according to the manufacturer's instructions. The cytokines with significant differences in expression were screened out.

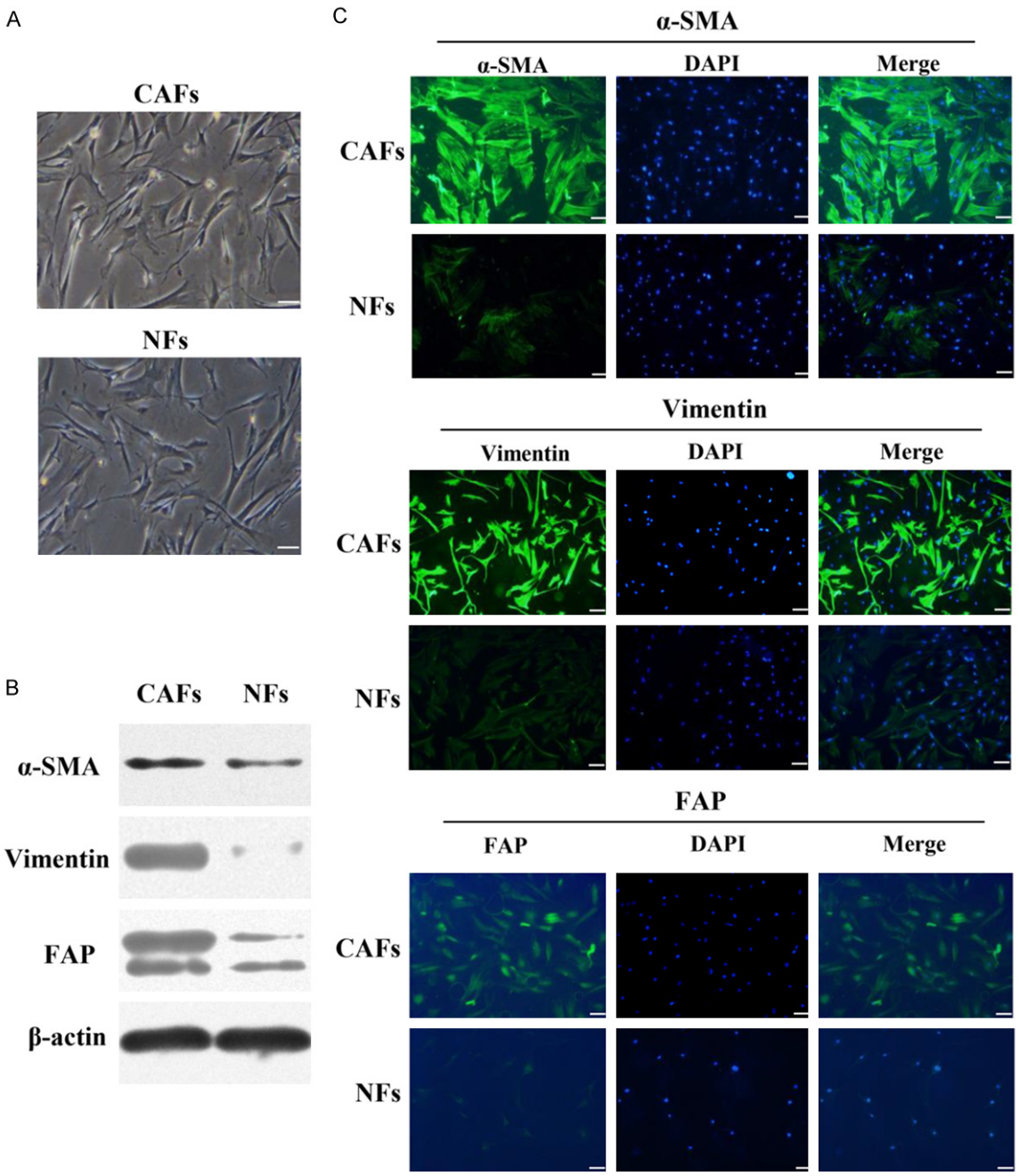

Figure S1. Characteristics of CAFs isolated from HCC patients. (A) Representative morphologies of CAFs and PTFs derived from HCC patients. Scale bar, 100 μm. (B and C) Expression levels of α-SMA, FAP, and vimentin in isolated fibroblasts were determined by western blot (B) and immunofluorescent staining (C). Scale bar, 100 μm. CAFs expressed higher levels of α-SMA, FAP, and vimentin than PTFs.

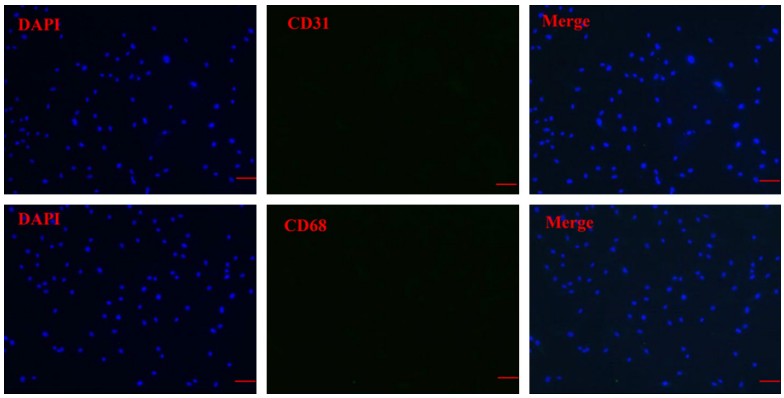

Figure S2. As assessed by immunofluorescent staining, the established CAFs showed negative expression for the endothelial marker CD31 and macrophage markers CD68. Scale bar, 100 μm.

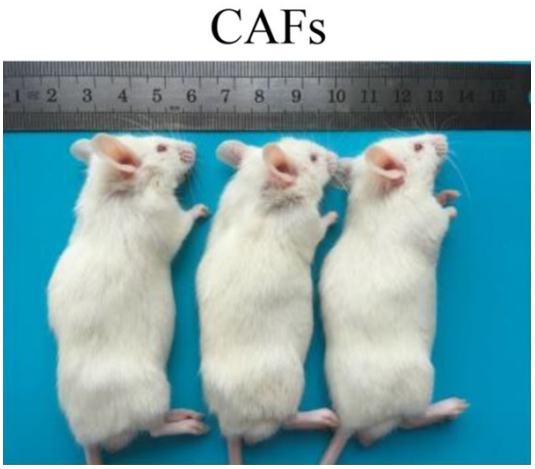

Figure S3. Detection of tumorigenesis of CAFs. CAFs (4×10^5) were injected into nude mice subcutaneously, and no tumors were detected in the mice after 35 days.

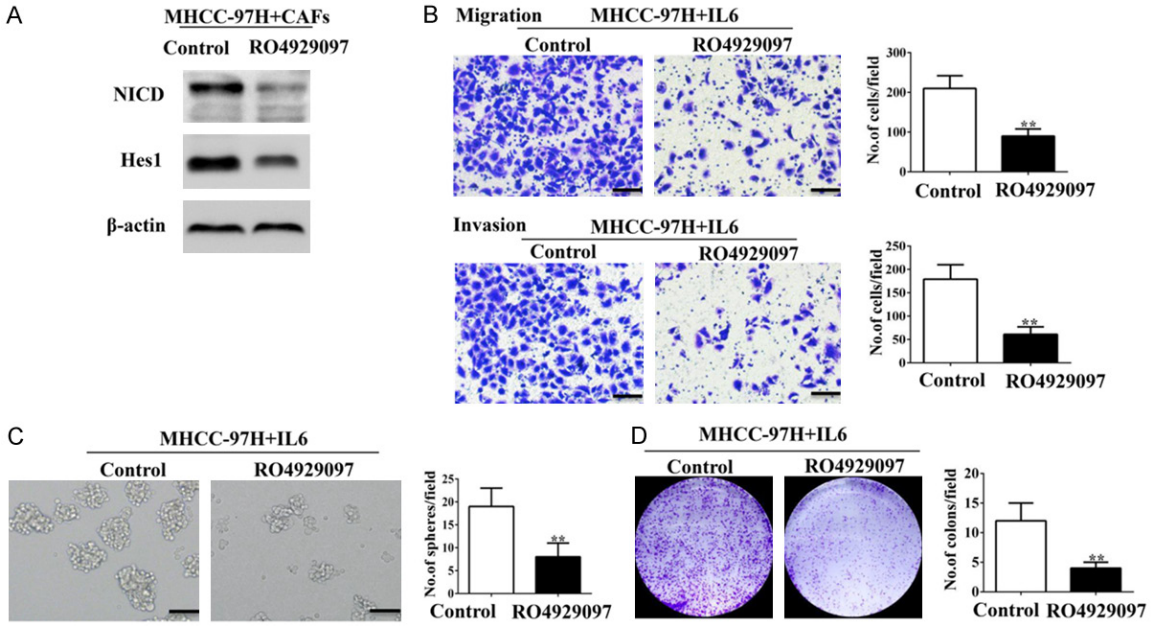

Figure S4. RO4929097 inhibited the CAFs-induced promotion of stem cell-like properties in HCC cells. RO4929097 suppressed the expression of Notch signaling-associated components (NICD, and Hes1) in MHCC-97H cells co-cultured with CAFs. (A) CAFs-induced migration, invasion (B) sphere-forming (C) and colony-forming (D), abilities of MHCC-97H cells decreased when Notch signaling was inhibited by RO4929097. Scale bar, 100μm. Data are shown as means ± SD from at least three independent experiments. (*P < 0.05, **P < 0.01).

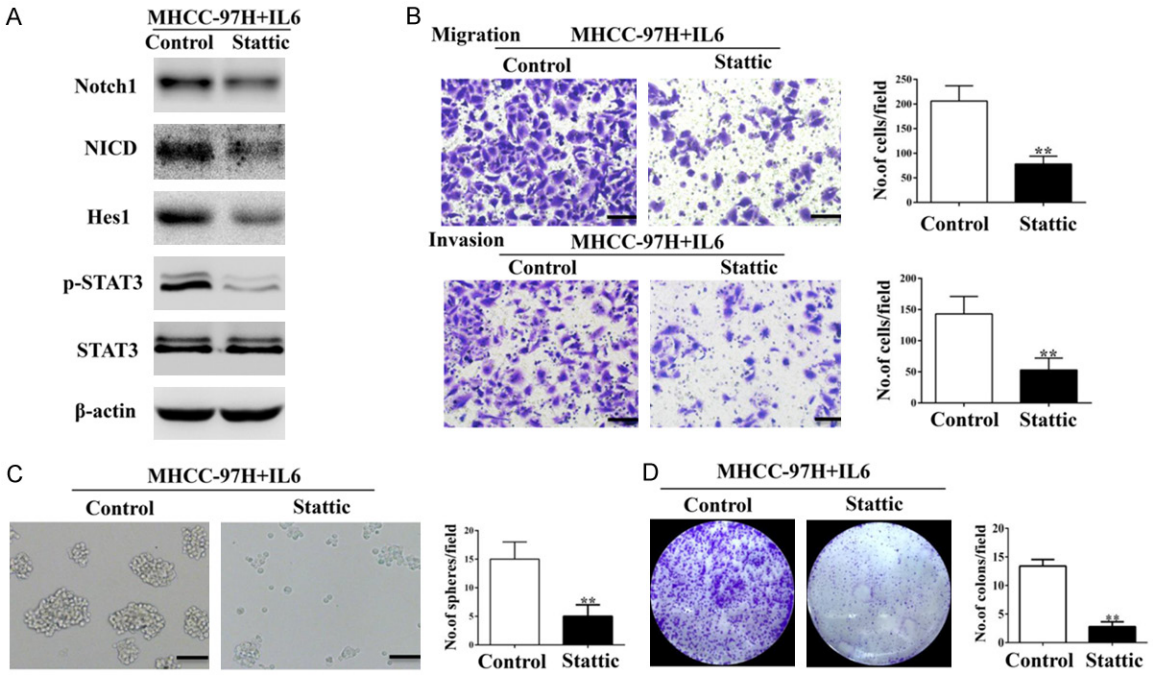

Figure S5. Stattic suppressed the expression of phospho-STAT3 and Notch signaling components (Notch1, NICD, and Hes1) in MHCC-97H cells treated with IL-6. (A) IL-6-induced migration, invasion (B) sphere-forming (C) and colony-forming (D), abilities of MHCC-97H cells decreased when STAT3 Tyr705 phosphorylation was inhibited by Stattic. Scale bar, 100μm. Data are shown as means ± SD from at least three independent experiments. (*P < 0.05, **P < 0.01).

Table S1. The correlation between α-SMA expression and nNICD expression in HCC patients

Variables	High α-SMA N=37	Low α-SMA N=51	*p* Value
Expression of nNICD			
Low	27	46	
High	10	5	P=0.034*

*P < 0.05, Signiicant difference, **P < 0.01, Signiicant difference (χ^2 test and Fisher's exact test).

Table S2. Tumor engraftment rates of HCC cells

Tumor engraftment rates of HCC cells which were injected into the subcutaneous tissue of NOD/SCID mice

Cell type	Cell numbers injected	Tumor incidence	Latency (days)[1]
CAFs	4×10^5	0/3	-
CAFs	2×10^5	0/3	-
CAFs	1×10^5	0/3	-
MHCC-97H cells	1×10^5	3/3	14
MHCC-97H cells	5×10^4	3/3	15
MHCC-97H cells	1×10^4	1/3	18
MHCC-97H cells +CAFs (1:1)	1×10^5	3/3	11
MHCC-97H cells +CAFs (1:1)	5×10^4	3/3	12
MHCC-97H cells +CAFs (1:1)	1×10^4	3/3	15
PLC/PRF/5 cells	1×10^5	2/3	15
PLC/PRF/5 cells	5×10^4	1/3	17
PLC/PRF/5 cells	1×10^4	0/3	-
PLC/PRF/5 cells +CAFs (1:1)	1×10^5	3/3	12
PLC/PRF/5 cells +CAFs (1:1)	5×10^4	3/3	14
PLC/PRF/5 cells +CAFs (1:1)	1×10^4	1/3	21

1, Approximate No. of days from tumor cell injection to the first appearance of tumors.

Tumor engraftment rates of HCC cells which were injected into the liver of NOD/SCID mice

Cell type	Cell numbers injected	Tumor incidence
shCtl-MHCC-97H cells	2×10^5	1/3
shCtl-MHCC-97H cells	1×10^5	0/3
shCtl-MHCC-97H cells	5×10^4	0/3
shCtl-MHCC-97H Cells + CAFs (1:1)	2×10^5	3/3
shCtl-MHCC-97H Cells + CAFs (1:1)	1×10^5	3/3
shCtl-MHCC-97H Cells + CAFs (1:1)	5×10^4	2/3

Cells + CAFs (1:1)		
shCtl-MHCC-97H	2×10^5	3/3
Cells + IL6		
shCtl-MHCC-97H	1×10^5	3/3
Cells + IL6		
shCtl-MHCC-97H	5×10^4	2/3
Cells + IL6		
shNOTCH1-MHCC-97H cells	2×10^5	1/3
shNOTCH1-MHCC-97H cells	1×10^5	0/3
shNOTCH1-MHCC-97H cells	5×10^4	0/3
shNOTCH1-MHCC-97H cells + CAFs (1:1)	2×10^5	3/3
shNOTCH1-MHCC-97H cells + CAFs (1:1)	1×10^5	0/3
shNOTCH1-MHCC-97H cells + CAFs (1:1)	5×10^4	0/3
shNOTCH1-MHCC-97H cells + IL6	2×10^5	1/3
shNOTCH1-MHCC-97H cells + IL6	1×10^5	0/3
shNOTCH1-MHCC-97H cells + IL6	5×10^4	0/3
MHCC-97H cells + IL6	2×10^5	3/3
MHCC-97H cells + IL6	1×10^5	2/3
MHCC-97H cells + IL6	5×10^4	2/3
MHCC-97H cells + IL6 + cryptotanshinone	2×10^5	0/3
MHCC-97H cells + IL6 + cryptotanshinone	1×10^5	0/3
MHCC-97H cells + IL6 + cryptotanshinone	5×10^4	0/3

Table S3. Sequences of primer

Gene	Sequences
Notch1	5’-CCGCAGTTGTGCTCCTGAA-3’
	5’-ACCTTGGCGGTCTCGTAGCT-3’
Hes1	5’-GCTAAGGTGTTTGGAGGCT-3’
	5’-CCGCTGTTGCTGGTGTA-3’
Nanog	5’-GTCCCAAAGGCAAACAACCC-3’
	5’-GCTGGGTGGAAGAGAACACA-3’
Sox2	5’-GCCCTGCAGTACAACTCCAT-3’
	5’-GACTTGACCACCGAACCCAT-3’
Oct4	5’-CTTGAATCCCGAATGGAAAGGG-3’
	5’-GACTTGACCACCGAACCCAT-3’
Fzd7	5’-GTGCCAACGGCCTGATGTA-3’
	5’-AGGTGAGAACGGTAAAGAGCG-3’
Gli1	5’-TGTGGGGACAGAAGTCAAGT-3’
	5’-GCCAATGGAGAGATGACCGT-3’
Smo	5’-CTGTCCTGCGTCATCATCTTT-3’
	5’-CCACAGCAAGGATTGCCAC-3’
β-actin	5’-GTTGCGTTACACCCTTTCTTG-3’
	5’-GACTGCTGTCACCTTCACCGT-3’
c-MYC	5’-GGCTCCTGGCAAAAGGTCA-3’
	5’-CTGCGTAGTTGTGCTGATGT-3’